Springer

KSME

Journal of Mechanical Science and Technology 32 (1) (2018) 433~445
www.springerlink.com/content/1738-494x(Print)/1976-3824(Online)
DOI 10.1007/s12206-017-1244-4

Performance assessment of turbular heat exchanger tubes containing rectangular-cut twisted tapes with alternate axes †

Anucha Saysroy, Wayo Changcharoen and Smith Eiamsa-ard*

Department of Mechanical Engineering, Mahanakorn University of Technology, Bangkok 10530, Thailand

(Manuscript Received March 2, 2017; Revised September 8, 2017; Accepted October 14, 2017)

Abstract

This paper describes the numerical results of the heat transfer enhancement mechanism of tubes containing rectangular-cut twisted tapes with alternate axes (ARC-TTs). Influence of the length of cut ratio ($LR = L/w$ = 2.0, 2.4 and 2.8) and width of cut ratio ($WR = W/w$ = 0.7, 0.8 and 0.9) on the heat transfer rate, friction factor and thermal performance characteristics are presented. The contour plots of predicted streamlines, velocity field, temperature field, and local Nusselt number distribution are also given for a better understanding of heat transfer mechanism. The results of the tube containing a classical twisted tape are also reported, for comparison. It can be observed that the use of ARC-TTs results in more disordered streamlines and higher turbulent intensity than that of the classical twisted tape. The numerical results also show that heat transfer and friction loss decrease as Length of cut ratio (*LR*) and Width of cut ratio (*WR*) increase while thermal performance factor shows reverse trend. In the studied range, utilizing ARC-TTs offers thermal performance factor up to 1.5.

Keywords: Rectangular-cut twisted tapes with alternate axes; Heat transfer enhancement; Swirling flow; Thermal performance

1. Introduction

Heat transfer enhancement (HTE) techniques refer to the improvement of thermohydraulic performance of heat exchangers. Since the past decade, the heat transfer enhancement techniques have been extensively applied in heat exchangers. Inserting a swirl/vortex generator into a heat exchanger tube is one of the most popular HTE techniques [1-12]. The technique has been applied in several thermal systems such as shell and tube heat exchanger, solar water heater, air conditioning and refrigeration systems, and chemical reactors, etc. Inserting twisted tape causes swirling flow as a secondary in bulk fluid. The swirling flow promotes the fluid mixing between core and wall regions, disturbs the thermal boundary layer and thus enhances heat transfer coefficient in existing system. Several attempts have been made to modify twisted tapes in order to improve heat transfer rate and/or to reduce pressure loss depending on application requirements. Ghadirijafarbeigloo et al. [8] used louvered twisted-tape inserts in a receiver tube of solar parabolic trough concentrator. The thermal performance factor of the tube with a louvered twisted-tape was enhanced up to 26 % as compared with that of the one with a classical twisted tape. Nanan et al. [11] compared heat transfer enhancement by a common helical twisted-tape and perforated helical twisted-tape inserts and found that perforated helical twisted-tapes caused lower friction loss at similar operating conditions. Piriyarungrod et al. [13] reported the effect of the tapered twisted tapes on heat transfer enhancement characteristics in a circular tube. Their results indicated that heat transfer enhancement increased with decreasing taper angle and twist ratio. Chokphoemphun et al. [14] studied the heat transfer and pressure loss characteristics in tubes with multiple twisted-tape inserts (Double, triple and quadruple tapes) in co and counter arrangements (Co/counter clockwise). Among the studied inserts, the quadruple counter-twisted tape insert provided the maximum thermal performance.

Recently, Tamna et al. [15] employed double twisted tapes in common with 30° V-shape ribs in a round tube. V-shape ribs with different relative rib heights were employed. Their results showed that the heat transfer and pressure drop increased with increasing rib height. Yongsiri et al. [16] studied the heat transfer and friction factor and thermal performance characteristic in a uniform heat flux tubes containing helically twisted tapes with alternate axes. Tapes with different tape pitch to tube diameter ratios (P/D = 1.0, 1.5 and 2.0) and alternate length to pitch length ratios (l/P = 1.0, 1.5 and 2.0) were utilized. As compared to a common helically twisted tape, the helically twisted tapes with alternate axes gave

*Corresponding author. Tel.: +662 9883666, Fax.: +662 9883666
E-mail address: smith@mut.ac.th
† Recommended by Associate Editor Ji Hwan Jeong

higher heat transfer rate and thermal performance factor. Singh et al. [17] reported the heat transfer rate and friction factor behaviors of roughened tubes with twisted tape inserts. Under constant pumping power criterion, the thermal performance of the roughened tube fitted with twisted tape was as high as 1.61 times of those of a plain tube. Khatua et al. [18] examined the heat transfer in horizontal tubes inserted with perforated twisted tapes in a condensation process of pure R-245fa vapor. They could observe that the use of perforated twisted tapes resulted in heat transfer enhancement up to 37.5 % over those of a plain. Eiamsa-ard et al. [19] investigated the heat transfer enhancement in a three-start spirally twisted tube inserted with triple-channel twisted tape at different tape width ratios (w/D = 0.1, 0.25, 0.34 and 0.5) and tube/tape arrangements (Belly-to-belly and belly-to-neck arrangements). Their results showed that the three-start spirally twisted tubes with twisted tapes in belly-to-neck arrangement at w/D = 0.1, 0.25 and 0.34 yielded higher heat transfer rate than the twisted tube alone up to 1.2 %, 21 % and 36 %, respectively. Saravanan et al. [20] determined the heat transfer characteristics in V-trough solar water heaters inserted with helix twisted tape, helix twisted tape with square cut and helix twisted tape with V-cut. They found that the heat transfer and frictional factor in case of the helix twisted tape with V-cut were higher than those found in case of the helix twisted tape with square cut. Changcharoen et al. [21] compared the effects of co/counter dual-twisted tapes and single twisted tape on heat transfer enhancement. At similar conditions, dual twisted tapes consistently gave higher heat transfer rates of the single one. Bhattacharyya et al. [22] numerically studied heat transfer enhancement of centre-trimmed twisted tapes with four different twist ratios of 1.0, 2.0, 3.0 and 4.0. They observed that the centre-cleared twin twisted tape with twist ratio of 1.0 gave the highest heat transfer rate and the best thermal performance. It was also mentioned that the effect of heat transfer enhancement was more important than the effect of friction increase. Early 2017, Saysroy and Eiamsa-ard [23] examined the enhancing heat transfer and thermal performance of tubes containing square cut twisted-tapes with different perforated width to tape width ratios (w/W = 0.5, 0.6, 0.7, 0.8 and 0.9) and perforated length to tape width ratios (L/W = 0.7, 0.8 and 0.9). The highest thermal enhancement factor of 1.37 was achieved by using square-cut twisted tapes at the largest perforated width to tape width ratio (w/W = 0.9) and the smallest perforated length to tape width ratio (L/W = 0.7). Man et al. [24] performed experiments to study the heat transfer and friction factor in dual-pipe heat exchangers mounted with alternation of clockwise and counterclockwise twisted tape and also a typical twisted tape. Their results showed that the alternation of clockwise and counterclockwise twisted tape gave higher heat transfer rate than the typical twisted tape, and gave thermal performance factor up to 1.42 over the plain tube under the same pumping power criterion. Hong et al. [25] investigated the influence of the spiral grooved tube inserted with twin overlapped twisted tapes with four overlapped twisted ratios (1.06, 1.56, 2.44 and 3.22). They found that Nusselt number and friction factor increased with decrease in the overlapped twisted ratio.

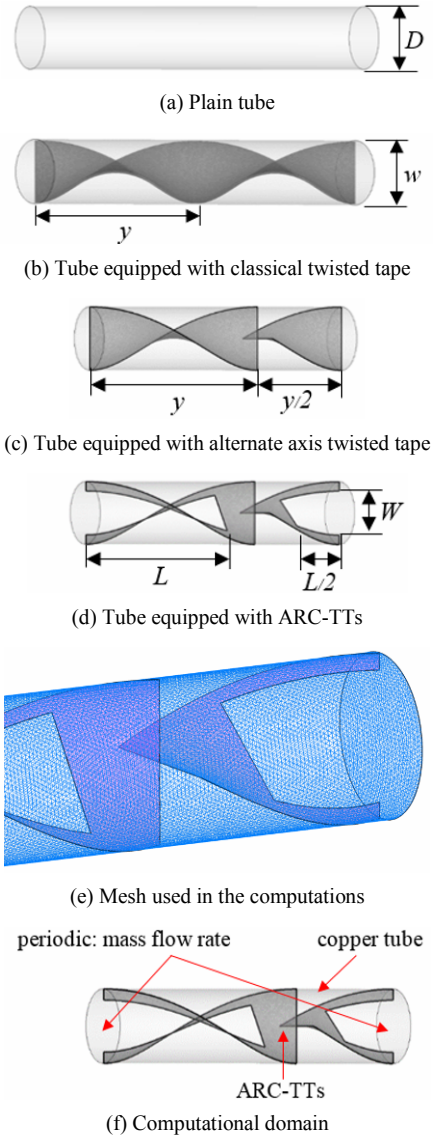

(a) Plain tube

(b) Tube equipped with classical twisted tape

(c) Tube equipped with alternate axis twisted tape

(d) Tube equipped with ARC-TTs

(e) Mesh used in the computations

(f) Computational domain

Fig. 1. Geometry of tubes with/without twisted tapes, mesh used in the computations, and computational domain of periodic flow.

The above literature review indicates that the heat transfer enhancement by using twisted tape inserts is strongly reliant on the geometry and arrangement of the inserts. For high heat transfer rate requirement, twisted tapes with special protruding parts (such as wings or ribs) and/or ones with small twist ratios and large surface area are preferred. For low friction loss penalty, twisted tapes with spaces or gaps are required. These two ideas have been combined to generate newly modified twisted tapes called rectangular-cut twisted tapes with alternate axes which are proposed in the present work. Rectangular-cuts form space while alternate axes promote flow fluctuation and thus turbulence intensity. In the present work, numerical study on the thermal and fluid flow, heat transfer,

friction, and thermal performance behaviors in the circular tubes containing rectangular-cut twisted tapes with alternate axes (ARC-TTs) has been carried out. The study encompassed the turbulent flow with Reynolds number (*Re*) ranging from 5000-15000 by using water as working fluid. Effects of length of cut ratios (*LR* = *L/w* = 2.0, 2.4 and 2.8) and width of cut ratios (*WR* = *W/w* = 0.7, 0.8 and 0.9) on heat transfer enhancement mechanism was analyzed. The plain tube with typical twisted tape were also examined for comparison.

2. Physical model and boundary conditions of alternate axis rectangular cut twisted tape inserts

The physical models of a plain tube, the tube containing twisted tape with alternate axis (A-TTs), the tube containing rectangular-cut twisted tape with alternate axis (ARC-TTs), mesh used in the computations, and computation domains are shown in Fig. 1. All tubes have the same inner diameter (*D*) of 14.5 mm (*w*). A tape twist ratio (*y/w*) is kept constant at 3.0. The computations are carried out with the following assumptions:

- The periodic boundaries are applied at the inlet and outlet of the flow domain (Velocity, and pressure gradients were in repetitive patterns).
- Water as the working fluid is assumed to be incompressible.
- The working fluid enters the tube at an inlet temperature (T_{in}) of 300 K (Pr = 5.86).
- A mass flow rate of water depending on the present Reynolds number value for the fully-developed periodic flow model.
- The physical properties of water remain constant based on average bulk temperature.
- The constant heat-flux of 600 W/m^2 is imposed on tube wall.
- A twisted tape is subjected to an adiabatic wall condition. The twisted tape was acted as the insulator (High thermal resistance). It is assumed that the material of twisted tape possesses low thermal conductivity (*e.g.* Plastics or acrylic).

3. Mathematical model and numerical method

3.1 Governing equations

The governing partial differential equations applied for the 3−D numerical simulations in the present work are shown as follow below.

Continuity equation:

$$\frac{\partial}{\partial x_i}\left(u_i\right)=0\,. \tag{1}$$

Momentum equation:

$$\frac{\partial}{\partial x_j}\left(\rho u_i u_j\right)=-\frac{\partial p}{\partial x_i}+\frac{\partial}{\partial x_j}\left[\mu\left(\frac{\partial u_i}{\partial x_j}-\rho\overline{u_i'u_j'}\right)\right]. \tag{2}$$

Energy equation:

$$\frac{\partial}{\partial x_j}\left(\rho u_i T\right)=\frac{\partial}{\partial x_j}\left(\left(\Gamma+\Gamma_t\right)\frac{\partial T}{\partial x_j}\right) \tag{3}$$

where Γ and Γ_t are molecular thermal diffusivity and turbulent thermal diffusivity, respectively. The diffusivities can be written as

$$\Gamma=\frac{\mu}{\mathrm{Pr}}\ \text{ and }\ \Gamma_t=\frac{\mu_t}{\mathrm{Pr}_t}\,. \tag{4}$$

For Reynolds averaged Navier-Stokes (RANS) equation, the Reynolds stresses, $-\rho\overline{u_i'u_j'}$ in Eq. (2) needs to be modeled. The Boussinesq hypothesis relates the Reynolds stresses to the mean velocity gradients as shown in the following equation:

$$-\rho\overline{u_i'u_j'}=\mu_t\left(\frac{\partial u_i}{\partial x_j}+\frac{\partial u_j}{\partial x_i}\right)-\frac{2}{3}\left(\rho k+\mu_t\frac{\partial \mu_k}{\partial x_k}\right)\delta_{ij} \tag{5}$$

where k is turbulent kinetic energy, defined by $k=1/2\cdot\overline{u_i'u_i'}$ and δ_{ij} is a Kronecker delta. The advantage in using Boussinesq approach is the relatively low computational cost for the computation of the turbulent viscosity, μ_t given as $\mu_t=\rho C_\mu k^2/\varepsilon$. The RNG k-ε model is one of the two-equation models that employ the Boussinesq hypothesis. The steady state transport equations can be expressed as:

$$\frac{\partial}{\partial x_i}\left(\rho k u_i\right)=\frac{\partial}{\partial x_j}\left(\alpha_k\mu_{eff}\frac{\partial k}{\partial x_j}\right)+G_k-\rho\varepsilon \tag{6}$$

$$\frac{\partial}{\partial x_i}\left(\rho\varepsilon u_i\right)=\frac{\partial}{\partial x_j}\left(\alpha_\varepsilon\mu_{eff}\frac{\partial \varepsilon}{\partial x_j}\right)+C_{1\varepsilon}\frac{\varepsilon}{k}G_k-C_{2\varepsilon}\rho\frac{\varepsilon^2}{k}-R_\varepsilon\,. \tag{7}$$

As above, α_k and α_ε are the inverse effective Prandtl number for k and ε, respectively. $C_{1\varepsilon}$ and $C_{2\varepsilon}$ are constants. G_k is the rate of TKE generation which can be expressed as:

$$G_k=-\rho\overline{u_i'u_j'}\frac{\partial u_j}{\partial x_i}\,. \tag{8}$$

The effective viscosity μ_{eff} is written by

$$\mu_{eff}=\mu+\mu_t=\mu+\rho C_\mu\frac{k^2}{\varepsilon} \tag{9}$$

where C_μ is a constant and set to 0.0845, derived using the ‘‘Renormalization group” (RNG) method.

In the present work, the turbulence models (Renormalized

Table 1. Summary of total numbers of elements.

-	*Number of elements*		
	LR = 2.0	*LR* = 2.4	*LR* = 2.8
Plain tube	905920		
Typical twisted tape	877330		
Alternated axis TT	747706		
ARC-TT, WR = 0.7	771680	768178	768069
ARC-TT, WR = 0.8	819224	818800	818278
ARC-TT, WR = 0.9	906430	905204	905049

group (RNG) $k-\varepsilon$, the standard $k-\varepsilon$, the standard $k-\omega$, and Shear stress transport (SST) k-ω turbulent models) have been selected. The numerical results were compared with those obtained from Manglik and Bergles correlations [26]. The governing equations are solved by using a finite volume approach and the SIMPLE algorithm. The time−independent incompressible Navier−Strokes equations and the turbulent model are discretized using the finite volume method. The standard pressure and QUICK (Quadratic upstream interpolation for convective kinetics differencing scheme) for momentum and energy equations are employed in the numerical model. The pressure−velocity coupling is handled by the SIMPLE (Semi implicit method for pressure−linked equations). The solutions are considered to be converged when the residuals of the continuity and momentum equations are less than 10^{-5} and that of the energy equation is less than 10^{-9}. The numerical simulation for the turbulent tubes fitted with rectangular-cut twisted tape with alternate axis (ARC-TTs) was performed using finite volume method.

3.2 Grid independent

A grid independence procedure is implemented by using the Richardson extrapolation technique over grids with different cell numbers. The tetrahedral grid (Fig. 1(e)) is used for meshing. In order to validate the solution independency of the grid number, five different grid numbers: 125123, 226528, 498520, 771680, 1143520 and 2071542 for ARC-TT with Width of cut ratio (*WR*) of 0.7, Length of cut ratio (*LR*) of 2.0 and twist ratio (y/w) of 3.0 at Reynolds number of 5000 by using the RNG k-ε turbulent model are comparatively evaluated. The predicted averaged Nusselt numbers for the five grid systems are shown in Fig. 2 for ARC-TT with *WR* = 0.7 and *LR* = 2.0. It was found that the average heat transfer (*Nu*) and friction factor (*f*) differences obtained at spaced meshes of 771680 and 114520 are less than 0.3 % and 0.6 %, respectively. Hence, the 771680 mesh element number is selected as a reference mesh size. The total numbers of elements used for plain tube, classical twisted tape, alternated axis twisted tape and rectangular-cut twisted tapes with alternate axes (ARC-TTs) at different width of cut ratios (*WR* = 0.7, 0.8 and 0.9) and length of cut ratios (*LR* = 2.0, 2.4 and 2.8) are presented in Table 1. In the present work, $y+$ values are below 3.5.

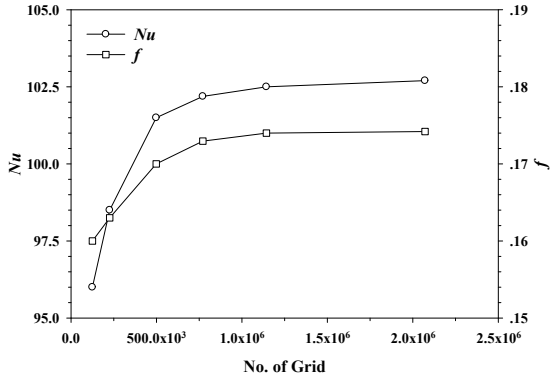

Fig. 2. Results of grid independence test for ARC-TT with *WR* = 0.7 and *LR* = 2.0.

3.3 Numerical analysis

The evaluation of heat transfer enhancement involves the dimensionless parameters described below. Reynolds number (Re) can be expressed as

$$Re = \frac{\rho \bar{u} D}{\mu}. \tag{10}$$

Friction factor (f) is computed using the following equation:

$$f = \frac{2D\Delta P}{\rho L \bar{u}^2}. \tag{11}$$

For the local Nusselt number (Nu_x), x is referred to the length from the surface boundary to the local point of interest which can be obtained from Eq. (12)

$$Nu_x = \frac{h_x D}{k}. \tag{12}$$

Average Nusselt number (Nu) is obtained by integrating the local Nusselt numbers (Nu_x) over the heat transfer area as

$$Nu = \frac{1}{A}\int Nu_x \partial A. \tag{13}$$

Thermal enhancement factor (TEF) is defined as the ratio of the Nusselt number ratio to the friction factor ratio for the uses of the tubes with twisted tape inserts and the plain tube (p) at an identical pumping power:

$$TEF = \frac{\left(Nu / Nu_p\right)}{\left(f / f_p\right)^{1/3}}. \tag{14}$$

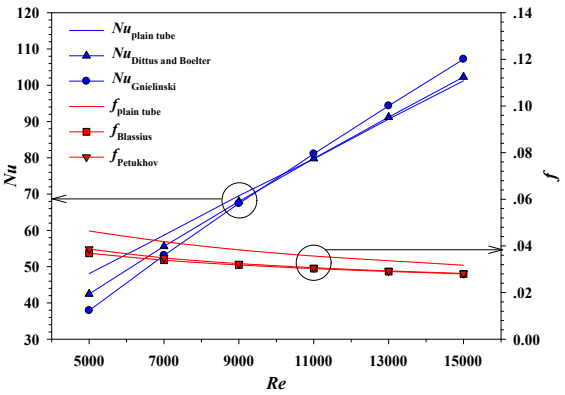

Fig. 3. Validation test of the plain tube.

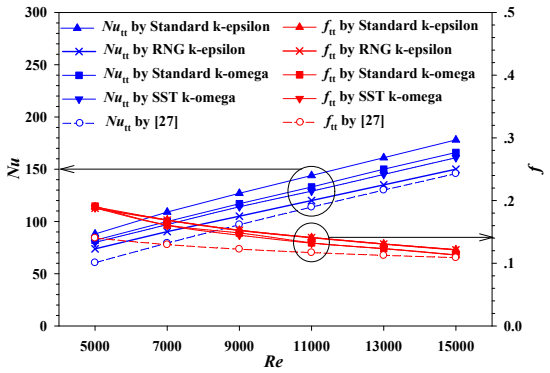

Fig. 4. Validation test of the tube inserted with twisted tape.

4. Result and discussion

4.1 Verification of the numerical method

The setup and numerical method were validated by comparing the present numerical results (Nusselt number and friction factor) of the plain tube with the data of the plain tube obtained from the standard correlations which are available in the open literature by Incropera et al. [27]. The Dittus-Boelter, Gnielinski, Petukhov and Blasius equations are the standard empirical correlations which is highly recommended for the result validation of a circular smooth tube [27]. The validation was performed for Reynolds numbers (*Re*) from 5000-15000. Evidently, both numerical Nusselt number and friction factor results were in good agreements with the correlation ones with small deviations. Fig. 3 shows that the present numerical Nusselt numbers deviate from Gnielinski correlation and Dittus-Boelter correlation within ±12 % and ±6.5 %, respectively while friction factors deviate from those obtained from Blasius correlation and Petukhov correlation within ±11.5 % and ±9 %, respectively. Therefore, the numerical method applied in the present work has a reasonable reliability.

Fig. 4 shows the comparison of the numerical Nusselt numbers and friction factors of the circular tube with twisted tape obtained from different turbulent models with those obtained from Manglik and Bergles correlation [26]. The correlations of Manglik and Bergles are the experimental results obtained under similar conditions as compared to those of the present investigation. Therefore, the correlations of Manglik and Bergles are used as the standards for validation of the present numerical results (Nusselt number, *Nu* and friction factor, *f*) as shown in Fig. 7. According to the results shown in Fig. 6, the deviations of the Renormalized group *k*-ε, the standard k-ε, the standard k-ω, and the Shear stress transport *k*-ω turbulent models were found to be 11.8 %, 13.8 %, 15.1 % and 18.5 % for the Nusselt number and 14.5 %, 15.1 %, 15.42 % and 14.6 % for friction factor, respectively. The deviations between the present and previous correlation [26] may be attributed to the experimental measurement uncertainties and the unavoidable discrepancies between the numerical methods and correlations. Among the tested model, RNG *k*-ε turbulent model shows the most accurate predictions as compared to those of previous correlation [26]. Therefore, the RNG *k*-ε turbulent model was subsequently applied for the Nusselt number and friction factor computations of a tube fitted with typical twisted tapes. These results indicate that the numerical data are sufficiently accurate and the present numerical method is reliable.

4.2 Flow structure, velocity field, temperature field and local Nusselt number distribution

The predicted results of the flow structure, velocity field, temperature field and local Nusselt number distribution in tubes with and without twisted tapes, at Reynolds number of 5000 as an example are shown in Figs. 5-8. The effects of length of cut ratio (*LR* = *L*/*w*) and width of cut ratio (*WR* = *W*/*w*) of rectangular-cut twisted tapes with alternate axes (ARC-TTs) are also reported. The temperature streamline shown in Fig. 5. Evidently, only axial flow is found in the plain tube while swirl flow as the secondary flow are detected in all tubes with twisted tape inserts. Swirl flow promotes mass and heat transfer from the central core to the near-wall region and vice versa. Obviously, the stream lines associated with the use of alternate axis twisted tape (A-TTs) and rectangular-cut twisted tapes with alternate axes (ARC-TTs) are more disordered than that with the use of the typical one. This is due to the flow fluctuation and fluid interrupting/mixing caused by the alternate axis while the high swirl and fluid mixing is found for alternate axis twisted tape (A-TTs) than those ARC-TTs. It is also found that the flow through ARC-TTs with larger Length of cut ratio (*LR*) and Width of cut ratio (*WR*) possesses lower swirl intensity than those with the smaller ones. The velocity fields shown in Fig. 6. Obviously, the high-speed flow region appears in the central part of the plain tube while tube with typical twisted tape (TT) inserted is divided into two parts and four parts for rectangular-cut twisted tapes with alternate axes (ARC-TTs). However, the ARC-TTs with largest length of cut ratio (*LR* = 2.8) and width of cut ratio (*WR* = 0.9) provide lower strange velocity field than other ARC-TTs due to the small protrusions into the flow stream. The fluctuation is reflected by non-uniform velocity

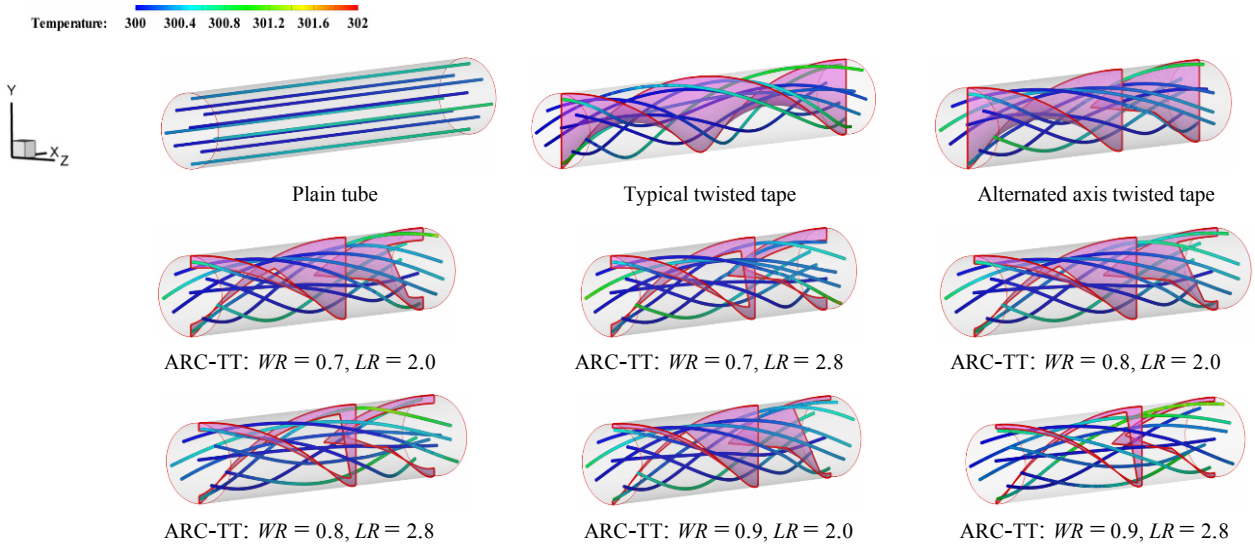

Fig. 5. Contour plot of temperature streamline of tubes with/without twisted tapes at Re = 5000.

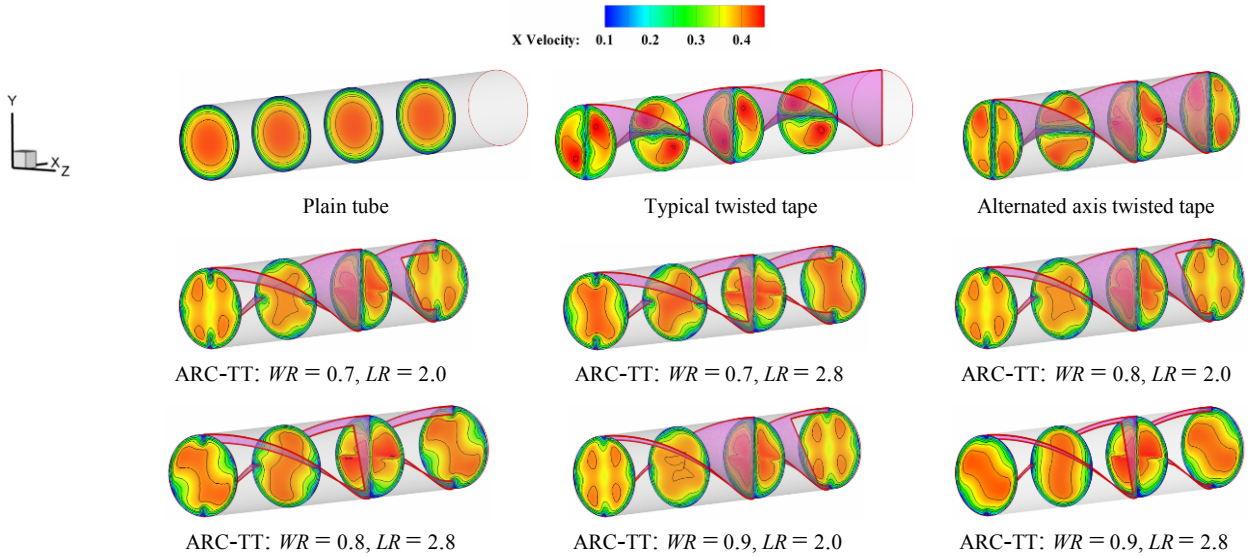

Fig. 6. Contour plot of velocity field at x/D = 0.0, 1.5, 3.0 and 4.5 of tubes with/without twisted tapes at Re = 5000.

contour throughout the tubes with alternate axis twisted tape and ARC-TTs. With the help of swirling flow and flow fluctuation, cold fluid is more efficiently transferred and contacted with tube wall (Hot surface), indicated by the thinner thermal boundary layers (Fig. 7).

The temperature fields shown in Fig. 7 demonstrate that, as the Length of cut ratio (LR) and Width of cut ratio (WR) increases, the thermal boundary layer becomes thicker due to the smaller effect of the swirl intensity especially at near the tape. Fig. 8 shows that alternated axis twisted tape and ARC-TTs yield considerably higher Nusselt number than the typical twisted tape. For ARC-TTs, swirling effect is diminished as Length of cut ratio (LR) and Width of cut ratio (WR) increase since more fluid flow directly through tape spaces. Consequently, heat transfer become poorer with increasing Length of cut ratio (LR) and Width of cut ratio (WR). Although the ARC-TT with the largest Length of cut ratio (LR = 2.8) and Width of cut ratio (WR = 0.9) provides the lowest heat transfer as compared the other ARC-TTs, it gives higher heat transfer rate than the typical twisted tape. It can be explained that the alternate axes help to induce the abrupt change of the flow direction and consequently, increase turbulence intensity.

4.3 Average Nusselt number and Nusselt number ratio

Fig. 9(a) presents the heat transfer rate in term of average Nusselt number (Nu), as a function of Reynolds number for the tubes with rectangular-cut twisted tapes with alternate axes (ARC-TTs), twisted tapes with alternate axes (A-TTs) and typical twisted tape (TT). In general, Nusselt number increases as Reynolds number (Re) increases owing to the increase of swirl/turbulence intensity. At a given Reynolds

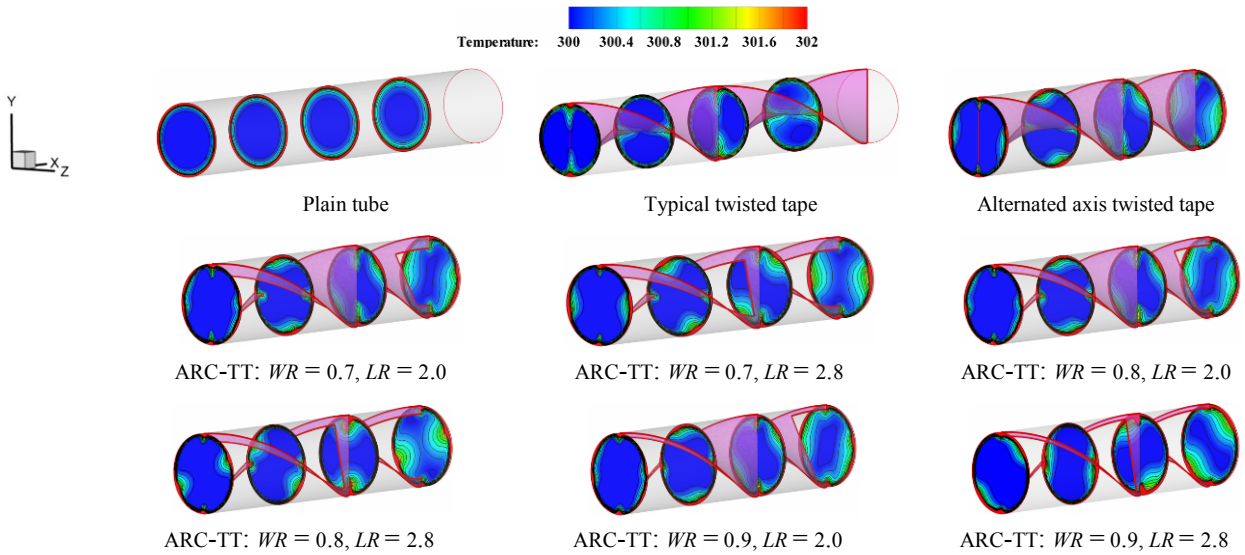

Fig. 7. Contour plot of temperature field at x/D = 0.0, 1.5, 3.0 and 4.5 of tubes with/without twisted tapes at Re = 5000.

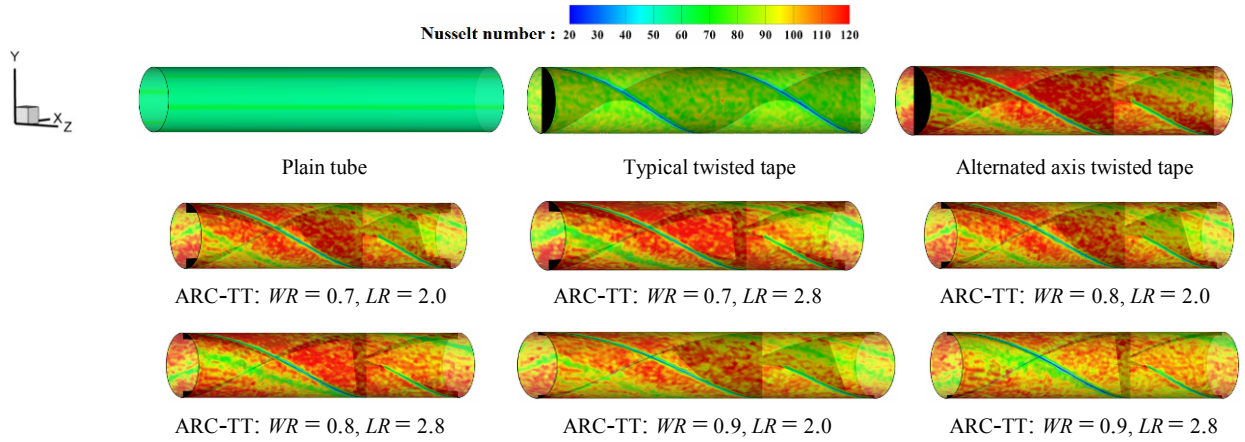

Fig. 8. Contour plot of Nusselt number distribution of tubes with/without twisted tapes at Re = 5000.

number, heat transfer rate of the flow in tubes with ARC-TTs/A-TTs/TT is considerable higher than that the plain tube. This is responsible by the swirl/turbulence induction by the ARC-TTs/A-TTs/TT.

The variations of average Nusselt number (Nu) and Nusselt number ratio (Nu/Nu_p) with Reynolds number (Re) for various length of cut ratios ($LR = L/w$ = 2.0, 2.4 and 2.8) and width of cut ratios (WR = W/w = 0.7, 0.8 and 0.9) are also depicted in Fig. 9(b). Among the tested twisted tapes, the alternate Axis twisted tape (A-TT) gives the highest Nusselt number, followed by rectangular-cut twisted tapes with alternate axes (ARC-TTs) and then the typical twisted tape (TT). The higher Nusselt numbers given by alternate axis twisted tape and ARC-TTs as compared to that given by the typical twisted tape, are due to the flow fluctuation effect/abrupt change of the flow direction as stated in Subsec. 4.2. The Nusselt number ratio ranges of the tubes with typical twisted tape (TT), alternate axis twisted tape (A-TT), and rectangular-cut twisted tapes with alternate axes (ARC-TTs) are 1.31-1.71, 1.87-2.17 and 1.71-2.13, respectively. For ARC-TTs, at similar condition Nusselt number tends to increase as Length of cut ratios (LR) decreases and Width of cut ratio (WR) decreases as clearly seen in Fig. 9(c). As compared to the alternate axis twisted tape (A-TT), the rectangular-cut twisted tapes with alternate axes (ARC-TTs) with WR = 0.7, 0.8 and 0.9 give 3.59-3.77 %, 4.11-9.23 % and 6.04-8.6 % lower Nusselt numbers, respectively. However, as compared to the typical twisted tape (TT), the rectangular-cut twisted tapes with alternate axes (ARC-TTs) with WR = 0.7, 0.8 and 0.9 give 22.86-38.85 %, 19.82-37.88 % and 14.68-35.76 % higher Nusselt numbers, respectively.

4.4 Average friction factor and friction factor ratio

The variation of the pressure drop in terms of friction factor as a function of Reynolds number is depicted in Figs. 10(a)-(c). Apparently, the presence of rectangular-cut twisted tapes with alternate axes (ARC-TTs), twisted tapes with alternate

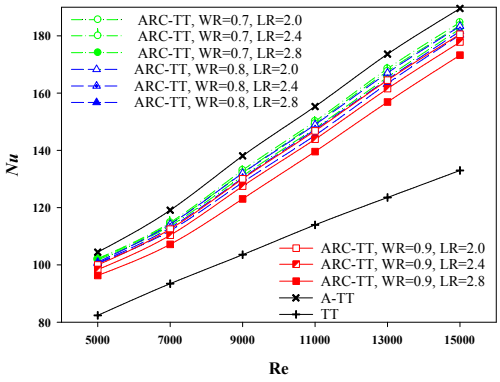

(a)

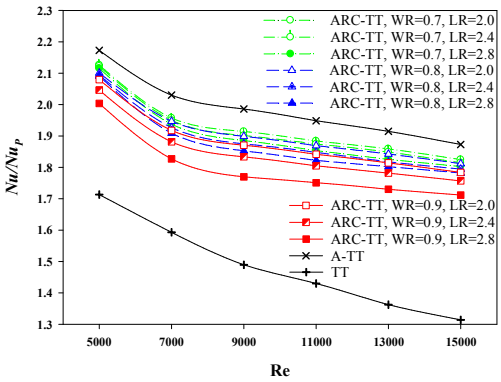

(b)

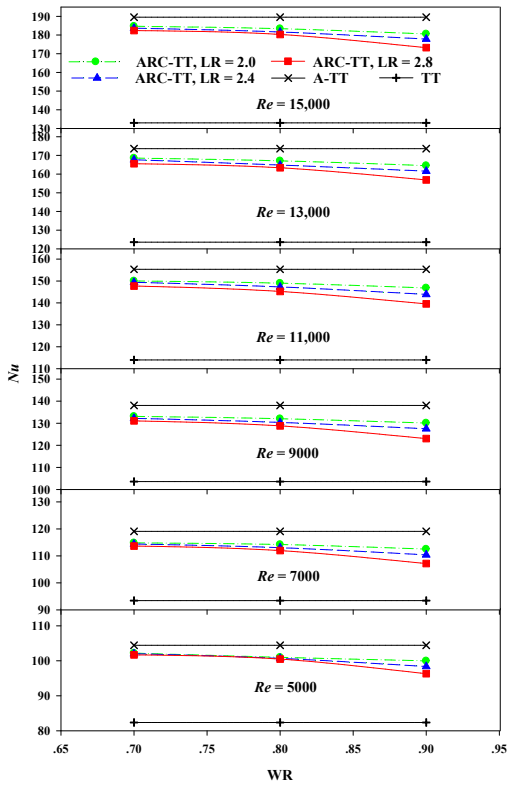

(c)

Fig. 9. Effects of Width of cut ratio (*WR*) and Length of cut ratio (*LR*) of ARC-TTs on Nusselt number.

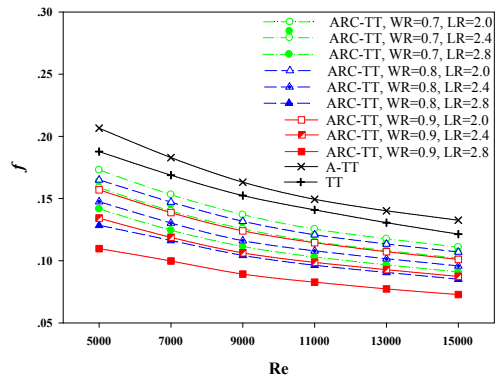

(a)

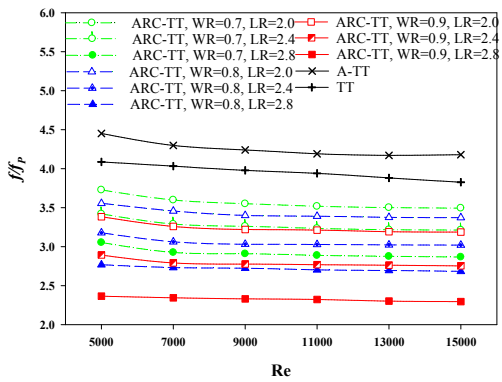

(b)

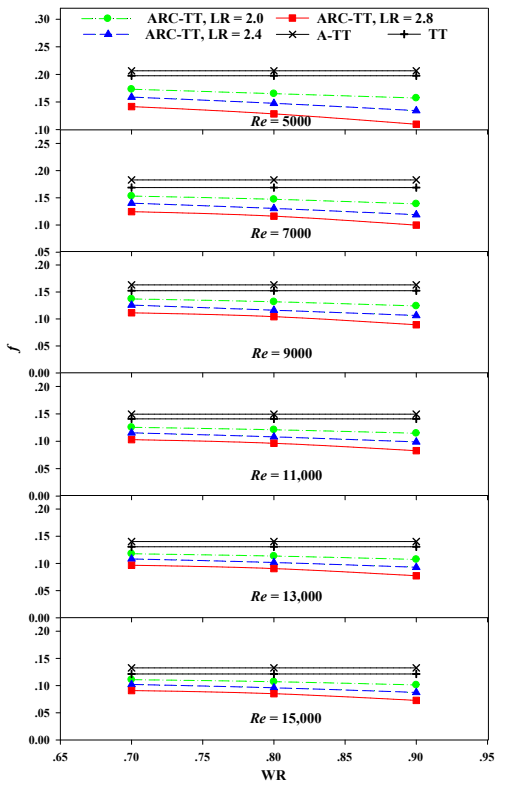

(c)

Fig. 10. Effects of Width of cut ratio (*WR*) and Length of cut ratio (*LR*) of ARC-TTs on friction factor.

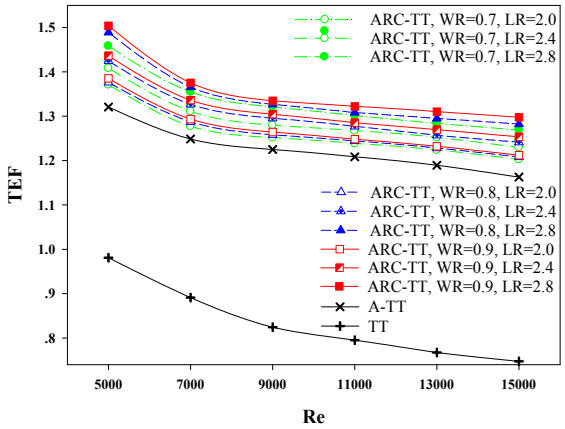

(a)

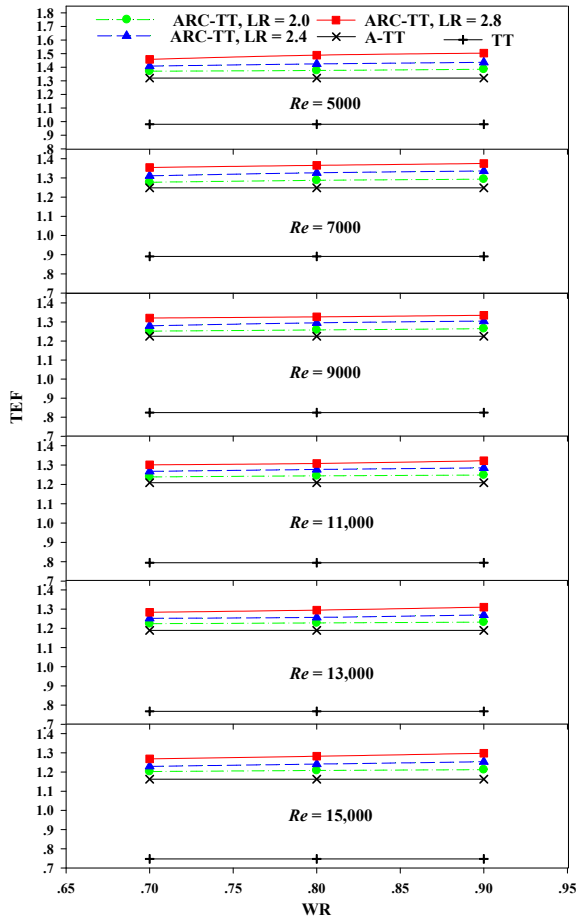

(b)

Fig. 11. Effects of Width of cut ratio (WR) and Length of cut ratio (LR) of ARC-TTs on thermal enhancement factor.

axes (A-TTs) and typical twisted tape (TT) causes significantly higher friction factor than that in the plain tube. For all cases, friction factor (*f*) gradually decrease with increasing Reynolds number. Because as Reynolds number increases, momentum overcomes the viscous force of the fluid and shear force between the fluid and the tube wall decreases.

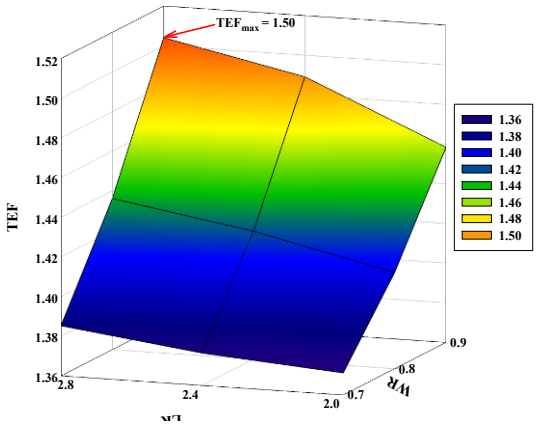

Fig. 12. The optimization of tube inserted with ARC-TTs at Re = 5000.

At similar conditions, friction factor decrease with increasing Length of cut ratio (*LR*) and Width of cut ratio (*WR*). Because rectangular-cut twisted tapes with alternate axes (ARC-TTs) with larger free spaces cause lower flow hindrance and obstruction. Besides, high friction loss is also caused by the strong turbulent fluctuation flow due to large area of contact between tapes and fluid. The friction factor ranges of the tubes with typical twisted tape (TT), alternate axis twisted tape and rectangular-cut twisted tapes with alternate axes are 3.86-4.5, 4.18-4.45 and 2.3-3.73, respectively. The rectangular-cut twisted tapes with alternate axes (ARC-TTs) with *WR* = 0.7, 0.8 and 0.9 cause 16.4-31.92 %, 19.08-37.83 % and 23.35-46.89 % lower friction factors than the alternate axis twisted tape (A-TT), respectively. In addition, as compared to the typical twisted tape (TT), the rectangular-cut twisted tapes with alternate axes (ARC-TTs) with *WR* = 0.7, 0.8 and 0.9 cause 8.71-28.26 %, 11.89-34.97 % and 16.73-44.44 % lower friction factors, respectively.

4.5 Thermal enhancement factor

Thermal enhancement factor (*TEF*) is very important aspect for operation of heat exchanger. In common, a *TEF* is evaluated under the same pumping power criterion, regarding to Eq. (16). Variation of thermal performance factor with Reynolds number for the tube with rectangular-cut twisted tapes with alternate axes (ARC-TTs), twisted tapes with alternate axes (A-TTs) and typical twisted tape (TT) is shown in Figs. 11(a) and (b). Mostly, thermal performance factors of modified twisted tape (ARC-TT/A-TTs) are over unity while the typical Twisted tape (TT) performs lower than unity especially at the high Reynolds number. Evidently, all rectangular-cut twisted tapes with alternate axes (ARC-TTs) give higher Thermal enhancement factor (*TEF*) than the twisted tapes with alternate axes (A-TTs) and typical twisted tape (TT) (Fig. 11) even though ARC-TTs give lower Nusselt number. The superior thermal performance of ARC-TTs is responsible by the lower friction loss. In other words, ARC-TTs offer better tradeoff between increased heat transfer and friction loss than the

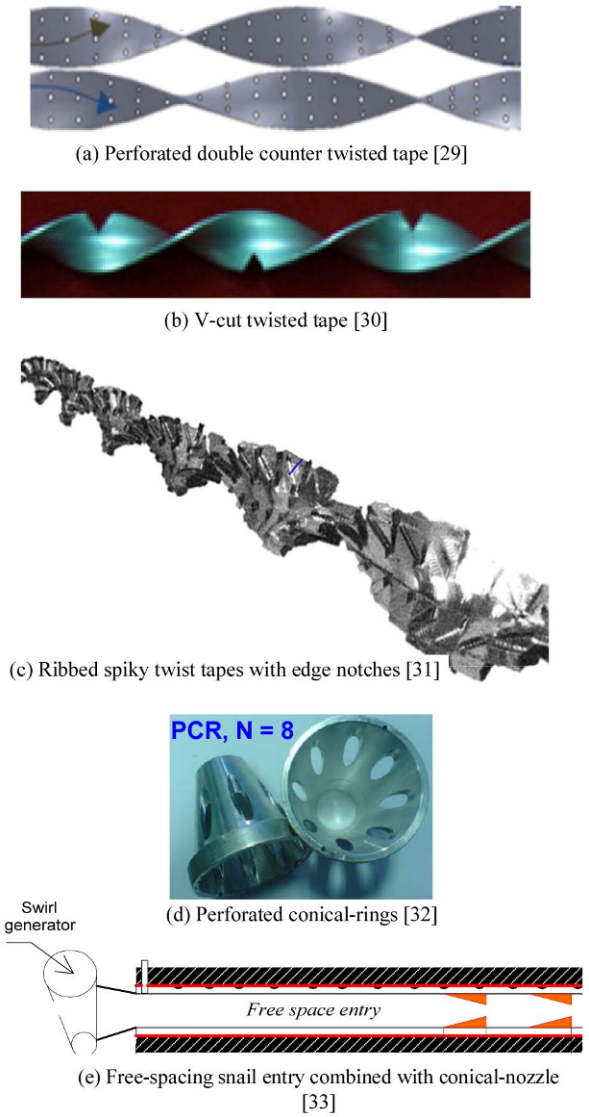

(a) Perforated double counter twisted tape [29]

(b) V-cut twisted tape [30]

(c) Ribbed spiky twist tapes with edge notches [31]

(d) Perforated conical-rings [32]

(e) Free-spacing snail entry combined with conical-nozzle [33]

Fig. 13. Photograph and picture view of the previously twisted tapes.

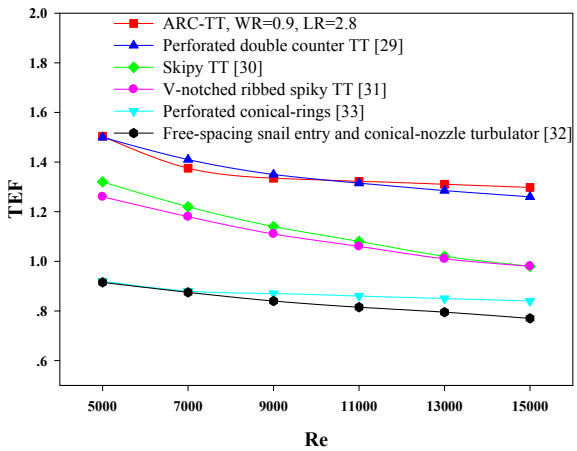

Fig. 14. Comparison of between thermal performance factors of ARC-TT in the present work and those of other previous works.

twisted tapes with alternate axes (A-TTs) and typical twisted tape (TT).

For ARC-TTs, Thermal enhancement factor (*TEF*) increases with increasing Length of cut ratio (*LR*) and Width of cut ratio (*WR*) (Figs. 11 and 12), primarily due to the lower friction loss. The Thermal enhancement factor (*TEF*) of the tubes with classical twisted tape, alternate axis twisted tape, and ARC-TTs are about 0.75-0.98, 1.16-1.32 and 1.2-1.5, respectively. As compared to the alternate axis twisted tape, ARC-TTs with *WR* = 0.7, 0.8 and 0.9 offer 3.41-10.41 %, 3.9-12.74 % and 4.25-13.87 % higher Thermal enhancement factor (*TEF*), respectively. For the range investigated, the maximum Thermal enhancement factor (*TEF*) of 1.5 is obtained by using the ARC-TT with *WR* = 0.9 and *LR* = 2.8 at the lowest Reynolds number of 5000 (Fig. 12). This implies that the rectangular-cut twisted tapes with alternate axes (ARC-TTs) are more suitable for practical application at lower Reynolds number at larger length of cut ratio and width of cut ratio.

For benchmarking, the Thermal performance factor (TEF) of the rectangular-cut twisted tapes with alternate axes (ARC-TTs) with the best thermal performance (*WR* = 0.9 and *LR* = 2.8) in the present study were compared with those in past study. The tapes subjected to the comparison include (1) perforated double counter twisted tape by Bhuiya et al. [28], (2) V-cut twisted tape by Murugesan et al. [29], (3) ribbed spiky twist tapes with edge notches by Chang and Huang [30], (4) free-spacing snail entry combined with conical-nozzle by Promvonge and Eiamsa-ard [31], and (5) perforated conical-rings by Kongkaitpaiboon et al. [32], as depicted in Fig. 13. The comparison of Thermal performance factors (*TEFs*) of the present and past studies is presented in Fig. 14.

Obviously, the Thermal performance factors (*TEF*) of the rectangular-cut twisted tapes with alternate axes (ARC-TTs) are superior to those of the V-cut twisted tape [29], ribbed spiky twist tapes with edge notches [30], free-spacing snail entry combined with conical-nozzle [31] and perforated conical-rings [32], since the rectangular-cut twisted tapes with alternate axes (ARC-TTs) possesses more effective heat transfer enhancement with low pressure loss. In addition, the rectangular-cut twisted tapes with alternate axes (ARC-TTs) give comparable thermal performance factor to the perforated double counter twisted tape [28]. In addition, the thermal performance factors of the rectangular-cut twisted tapes with alternate axes (ARC-TTs) are consistently better than those of the typical twisted tape (TT).

5. Conclusions

The heat transfer, friction factor and Thermal enhancement factor (*TEF*) characteristics of turbulent flow in the tubes containing rectangular-cut twisted tapes with alternate axes (ARC-TTs) with different Width of cut ratios (*WR*) and Length of cut ratios (*LR*) have been numerically investigated for Reynolds number ranging from 5000 to 15000. The simulations for the alternate axis twisted tape and classical twisted

tape have also been performed, for comparison. The major findings are concluded below.

- ARC-TTs as the modified twisted tapes give 14.68-38.85 % higher Nusselt numbers than the typical twisted tape but 2.16-10.88 % lower than the alternate axis twisted tape.
- ARC-TTs cause 8.71-44.44 % and 16.04-46.89 % lower friction factors than the typical twisted tape and the alternate axis twisted tape, respectively.
- Nusselt number and friction factor decrease with increasing Width of cut ratio (*WR*) and Length of cut ratio (*LR*).
- Thermal enhancement factor (*TEF*) increases with increasing Width of cut ratio (*WR*) and Length of cut ratio (*LR*). The maximum Thermal enhancement factor (*TEF*) of 1.5 is obtained by using the tube with *WR* = 0.9 and *LR* = 2.8 at the lowest Reynolds number of 5000.

Acknowledgements

The authors would like to acknowledge the software support from King Mongkut's Institute of Technology Ladkrabang (KMITL) and the help of Associate Professor Pongjet Promvonge and Associate Professor Jarruwat Charoensuk for their technical assistance on ANSYS FLUENT, particularly in the post processing of analysis results.

Nomenclature

A	: Heat transfer area on tube surface, m^2
$C_{1\varepsilon}$, $C_{2\varepsilon}$	: Turbulent model constant
C_μ	: Function of the mean strain and rotation rate
D	: Diameter of tube, m
f	: Friction factor
G_k	: Production of turbulence kinetic energy due to the mean velocity gradients, kg $s^{-2}m^{-1}$
h	: Heat transfer coefficient, W m^{-2} K^{-1}
k	: Thermal conductivity of fluid, W m^{-1} K^{-1} or Turbulent kinetic energy, m^2 s^{-2}
Nu	: Average Nusselt number
Nu_x	: Local Nusselt number
Nu/Nu_p	: Nusselt number of twisted tape to Nusselt number of plain tube
P	: Pressure, Pa
ΔP	: Pressure drop, Pa
Re	: Reynolds number
T	: Temperature, K
u	: Velocity component, m s^{-1}
$\overline{u}$	: Average velocity in the tube, m s^{-1}
u_i	: Velocity component in x_i-direction, m s^{-1}
u_i'	: Fluctuation velocity in x_i-direction, m s^{-1}
u_j	: Velocity component in x_j-direction, m s^{-1}
u_j'	: Fluctuation velocity in x_j-direction, m s^{-1}
x_i, x_j	: Coordinate direction
x	: x-position
y	: y-position
z	: z-position
w	: Tape width, m
y	: Pitch length of twisted tape, m
y/w	: Twist ratio

Greek Symbols

ρ	: Fluid density, kg m^{-3}
Γ	: Thermal diffusivity, kg s^{-1} m^{-1}
Γ_t	: Turbulent thermal diffusivity, kg s^{-1} m^{-1}
δ_{ij}	: Kronecker delta
ε	: Dissipation rate, m^2 s^{-3}
ω	: Specific rate of dissipation, s^{-1}
α_k	: Inverse effective Prandtl number for k, kg $s^{-2}m^{-1}$
α_ε	: Inverse effective Prandtl number for ε, kg $s^{-2}m^{-1}$
μ	: Fluid dynamic viscosity, kg s^{-1} m^{-1}
μ_{eff}	: Effective viscosity

Abbreviations

ARC−TT	: Rectangular−cut twisted tapes with alternate axes
A-TT	: Twisted tape with alternate axes
LR	: Length of cut ratio
RNG	: Renormalized group
SST	: Shear stress transport
TEF	: Thermal enhancement factor
TKE	: Turbulent kinetic energy, m^2 s^{-2}
TT	: Typical twisted tape
WR	: Width of cut ratio

Subscripts

eff	: Effective
p	: Plain tube
i, j, k	: Cartesian coordinates
t	: Turbulent

Superscripts

—	: Average

References

[1] S. D. Salman, A. A. H. Kadhum, M. S. Takriff and A. B. Mohamad, Numerical investigation of heat transfer and friction factor characteristics in a circular tube fitted with V-cut twisted tape inserts, *The Scientific World Journal,* ID 492762 (2013) 1-8.

[2] H. R. Kim, S. Kim, M. Kim, S. H. Park, J. K. Min and M. Y. Ha, Numerical study of fluid flow and convective heat transfer characteristics in a twisted elliptic tube, *Journal of Mechanical Science and Technology,* 30 (2016) 719-732.

[3] S. Eiamsa-ard, K. Yongsiri, K. Nanan and C. Thianpong, Heat transfer augmentation by helically twisted tapes as swirl and turbulence promoters, *Chemical Engineering and*

Processing: Process Intensification, 60 (2012) 42-48.

[4] W. Jedsadaratanachai and A. Boonloi, Thermal performance assessment in a fin-and-oval-tube heat exchanger with delta winglet vortex generators, *Journal of Mechanical Science and Technology,* 29 (2015) 1765-1779.

[5] S. Eiamsa-ard and W. Changcharoen, Flow structure and heat transfer in a square duct fitted with dual/quadruple twisted-tapes: Influence of tape configuration, *Journal of Mechanical Science and Technology,* 29 (2015) 3501-3518.

[6] S. Eiamsa-ard, Study on thermal and fluid flow characteristics in turbulent channel flows with multiple twisted tape vortex generators, *International Communications in Heat and Mass Transfer,* 37 (2010) 644-651.

[7] C. Thianpong, P. Eiamsa-ard and S. Eiamsa-ard, Heat transfer and thermal performance characteristics of heat exchanger tube fitted with perforated twisted-tapes, *Heat and Mass Transfer, Wärme- und Stoffübertragung,* 48 (2012) 881-892.

[8] Sh. Ghadirijafarbeiglooa, A. H. Zamzamianb and M. Yaghoubi, 3-D numerical simulation of heat transfer and turbulent flow in a receiver tube of solar parabolic trough concentrator with louvered twisted-tape inserts, *Energy Procedia,* 49 (2014) 373-380.

[9] P. Promvonge and S. Eiamsa-ard, Heat transfer and turbulent flow friction in a circular tube fitted with conical-nozzle turbulators, *International Communications in Heat and Mass Transfer,* 34 (2007) 72-82.

[10] C. Thianpong, P. Eiamsa-ard, P. Promvonge and S. Eiamsa-ard, Effect of perforated twisted-tapes with parallel wings on heat transfer enhancement in a heat exchanger tube, *Energy Procedia,* 14 (2012) 1117-1123.

[11] K. Nanan, C. Thianpong, P. Promvonge and S. Eiamsa-ard, Investigation of heat transfer enhancement by perforated helical twisted-tapes*, International Communications in Heat and Mass Transfer,* 52 (2014) 106-112.

[12] C. Nuntadusit, I. Piya, M. Wae-hayee and S. Eiamsa-ard, Heat transfer characteristics in a channel fitted with zigzag-cut baffles, *Journal of Mechanical Science and Technology,* 29 (2015) 2547-2554.

[13] N. Piriyarungrod, S. Eiamsa-ard, C. Thianpong, M. Pimsarn and K. Nanan, Heat transfer enhancement by tapered twisted tape inserts, *Chemical Engineering and Processing,* 96 (2015) 62-71.

[14] S. Chokphoemphun, M. Pimsarn, C. Thianpong and P. Promvonge, Thermal performance of tubular heat exchanger with multiple twisted-tape inserts, *Chinese Journal of Chemical Engineering,* 23 (2015) 755-762.

[15] S. Tamna, Y. Kaewkohkiat, S. Skullong and P. Promvonge, Heat transfer enhancement in tubular heat exchanger with double V-ribbed twisted-tapes, *Case Studies in Thermal Engineering,* 7 (2016) 14-24.

[16] K. Yongsiri, C. Thianpong, K. Nanan and S. Eiamsa-ard, Thermal performance enhancement in tubes using helically twisted tape with alternate axis inserts, *Thermophysics and Aeromechanics,* 23 (2016) 69-81.

[17] V. Singh, S. Chamoli, M. Kumar and A. Kumar, Heat transfer and fluid flow characteristics of heat exchanger tube with multiple twisted tapes and solid rings inserts, *Chemical Engineering and Processing: Process Intensification,* 102 (2016) 156-168.

[18] A. K. Khatua, P. Kumar, H. N. Singh and R. Kumar, Measurement of enhanced heat transfer coefficient with perforated twisted tape inserts during condensation of R-245fa, *Heat and Mass Transfer/Waerme- und Stoffuebertragung,* 52 (2016) 683-691.

[19] S. Eiamsa-ard, P. Promthaisong, C. Thianpong, M. Pimsarn and V. Chuwattanakul, Influence of three-start spirally twisted tube combined with triple-channel twisted tape insert on heat transfer enhancement, *Chemical Engineering and Processing: Process Intensification,* 102 (2016) 117-129.

[20] A. Saravanan, J. S. Senthilkumaar and S. Jaisankar, Performance assessment in V-trough solar water heater fitted with square and V-cut twisted tape inserts, *Applied Thermal Engineering,* 102 (2016) 476-486.

[21] W. Changcharoen, P. Samruaisin, P. Eiamsa-ard and S. Eiamsa-ard, Heat transfer characteristics of decaying swirl flow through a circular tube with co/counter dual twisted-tape swirl generators, *Thermophysics and Aeromechanics,* 23 (2016) 523-536.

[22] S. Bhattacharyya, H. Chattopadhyay and S. Bandyopadhyay, Numerical study on heat transfer enhancement through a circular duct fitted with centre-trimmed twisted tape, *International Journal of Heat and Technology,* 34 (2016) 401-406.

[23] A. Saysroy and S. Eiamsa-ard, Periodically fully-developed heat and fluid flow behaviors in a turbulent tube flow with square-cut twisted tape inserts, *Applied Thermal Engineering,* 112 (2017) 895-910.

[24] C. Man, X. Lv, J. Hu, P. Sun and Y. Tang, Experimental study on effect of heat transfer enhancement for single-phase forced convective flow with twisted tape inserts, *International Journal of Heat and Mass Transfer,* 106 (2017) 877-883.

[25] Y. Hong, J. Du and S. Wang, Experimental heat transfer and flow characteristics in a spiral grooved tube with overlapped large/small twin twisted tapes, *International Journal of Heat and Mass Transfer,* 106 (2017) 1178-1190.

[26] R. M. Manglik and A. E. Bergles, Heat transfer and pressure drop correlations for twisted-tape inserts in isothermal tubes: Part II-Transition and turbulent flows, *Transactions of the ASME Journal of Heat Transfer,* 115 (1993) 890-896.

[27] F. P. Incropera, P. D. Dewitt, T. L. Bergman and A. S. Lavine, *Fundamentals of heat and mass transfer,* John-Wiley & Sons (2006).

[28] M. M. K. Bhuiya, A. K. Azad, M. S. U. Chowdhury and M. Saha, Heat transfer augmentation in a circular tube with perforated double counter twisted tape inserts, *International Communications in Heat and Mass Transfer,* 74 (2016) 18-26.

[29] P. Murugesan, K. Mayilsamy, S. Suresh and P. S. S. Srini-

vasan, Heat transfer and pressure drop characteristics in a circular tube fitted with and without V-cut twisted tape insert, *International Communications in Heat and Mass Transfer,* 38 (2011) 329-334.

[30] S. W. Chang and B. J. Huang, Thermal performances of tubular flows enhanced by ribbed spiky twist tapes with and without edge notches, *International Journal of Heat and Mass Transfer,* 73 (2014) 645-663.

[31] P. Promvonge and S. Eiamsa-ard, Heat transfer in a circular tube fitted with free-spacing snail entry and conical-nozzle turbulators, *International Communications in Heat and Mass Transfer,* 34 (2007) 838-848.

[32] V. Kongkaitpaiboon, K. Nanan and S. Eiamsa-ard, Experimental investigation of heat transfer and turbulent flow friction in a tube fitted with perforated conical-rings, *International Communications in Heat and Mass Transfer,* 37 (2010) 560-567.

[33] S. Eiamsa-ard, P. Somklieng and C. Thianpong, Heat transfer enhancement in tube by inserting uniform/non-uniform twisted-tapes with alternate axes: Effect of rotated-axis length, *Applied Thermal Engineering,* 54 (2013) 289-309.

Anucha Saysroy is currently D.Eng. candidate at Mahanakorn University of Technology. He received his B. Eng. degree from Phetchaburi Rajabhat University and M. Eng. degree from King Mongkut's University of Technology North Bangkok, Thailand. He has been working at Phetchaburi Rajabhat University since 2012. His research interests include Computation Fluid Dynamics (CFD), heat transfer, fluid flow, and heat exchanger.

Wayo Changcharoen is Assistant Professor of Mechanical Engineering at Mahanakorn University of Technology (MUT), Thailand. He received D. Eng. at King Mongkut's Institute of Technology Ladkrabang in 2012. His current interests include heat transfer enhancement for jet impingement, channel with rib/baffle turbulators and CFD.

Smith Eiamsa-ard is an Associate Professor of Mechanical Engineering at Mahanakorn University of Technology (MUT), Thailand. He obtained his D.Eng. in Mechanical Engineering from King Mongkut's Institute of Technology Ladkrabang. He has been working at MUT since 1996. His research interests include heat transfer enhancement, swirling flow, impinging jet and heat exchanger.